TEORIJSKA I PRIMENJENA MEHANIKA 16, pp 25–38, 1990, UDK 539.3

# DETERMINATION OF THIN-WALLED CYLINDRICAL SHELLS STABILITY

*A. Crnjac & P. Crnjac*

(Recived 30.05.1990, revised 25.10.1990.)

**1. Introduction.** Shells are used either as independent elements or elements forming part of modern structures in all industrial fields. Shell load is dependent upon the loss of stability. For this reason special attention is paid to the problem of stability. During the last fifty years, a great many publications have been issued dealing with the stability of shells. The research results vary a great deal as mathematical problems, nonhomogeneity and anisotropy of material, inaccuracy of manufacture, in short, shell imperfection, cause the actual conditions to considerably differ from theoretical computations. Because of this, experiments are sometimes the only way for assessing the real state in the shell. The present paper shows the experimental test results of cylindrical shells compared with the theoretical computations. On the basis of such results a unique method for determining the critical force of cylindrical shells within both, the elastic and plastic ranges, is given without considering the factor of imperfection $\alpha$.

**2. Material, dimensions and manufacture of shells.** Shells have been made from low-carbon 0.4, 0.5 and 0.6 mm-thick sheet steel suitable for plastic deformation with diameters ranging from $D = 200$, 250, 300, 350, 400, 500, 550, 600, 650, 700, 750, 800, 850, 900, 950, to 1000 mm. Manufactured have been five samples per each diameter.

According to classical theory critical load of axially loaded cylindrical shell does not depend on its length. The tests have, nevertheless, shown that the shell length should be within the limits of

$$0.75D < L < 15D \tag{1}$$

where $D$ is shell diameter and $L$ shell length. With shells shorter than $0.75D$, boundary disturbances had an influence on the occurrence of critical force, whereas those longer than $15D$ behaved as tubular bars.

On hand of the limited size of machines shell lengths as follows have been chosen:

$$L = 1.4D. \tag{2}$$

Used for the manufacture of both, shells and pots has been the deep drawing procedure.

It is known that plastic deformations may hamper the physical properties of material and that through thermal treatment original state can be reestablished.

The results of tearing tests performed on test tubes cut from thermally treated pot have shown that physical properties of material have regained their normal limits and nearly reached the values the material had prior to deep drawing. The bottom has been cut from the pot on a special machine as well as the excess of material on the other side. As all interior local stresses resulting from plastic deformations have been destroyed through annealling, the shell maintained the same cylindrical shape after cutting as the original pot.

**3. Shell test.** The shell has been put between two massive plates so as to exclude any possibility of the plate to bend because of the axial load. Shell shape is shown in Fig. 1. The cylindrical part of plate $D_c$ with a diameter slightly larger than shell diameter has a centering function and at the same time it also creates the stiffness of the shell thus preventing the influence of boundary disturbances. Plate is of simple shape and is very practical for easy mounting and dismantling. Fig. 2 illustrates the shell ready for test.

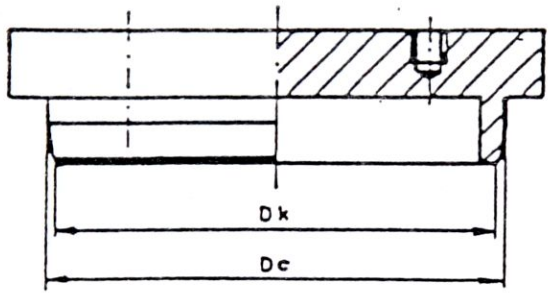


Fig. 1

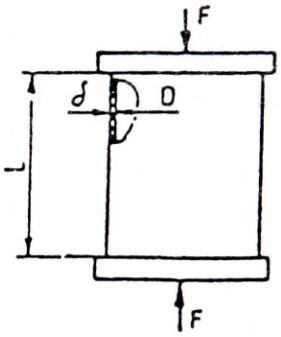


Fig. 2

$D_c = D + 0.15\delta$ — diameter of cylindrical part of plate
$D_k = D - \delta$ — diameter of conical part of plate
$D$ — shell interior diameter
$\delta$ — shell wall thickness
$L$ — shell length

In order to smooth out any possible nonparallelism between shell edges an articulated insert has been placed between the press plunger and the upper plate. Shell has been loaded with gradually increasing compression force. Throughout the test we have surveyed the shell surface in order to notice any changes in shape.

Deformations appeared on the shell after a particular load has been applied. With shells of larger diameters such deformations occurred in the form of a net of rhomboids. This happens instantaneously resulting in the establishment of a temporary state of balance in the shell. We shall call this state the UNSTABLE state and the force causing it the CRITICAL force.The state of the shell till the

the appearance of the critical force shall be called the STABLE condition. With the appearance of rhomboidal deformations the value of critical force has fallen by about 4%. By gradual removal of load, a shift from rhomboidal to plane surface has been noticed at a force lower by about 40% than the critical value. Gradual loading repeated, the phenomenon reappears at a critical force being lower by about 5% than the former one. With shells of smalller diameters the critical force has caused local deformations which have not disappeared once the load being removad from the shell.

**4. Test results.** Fig. 3 shows the measured values of critical forces $F_{cr}$ in the form of curves.

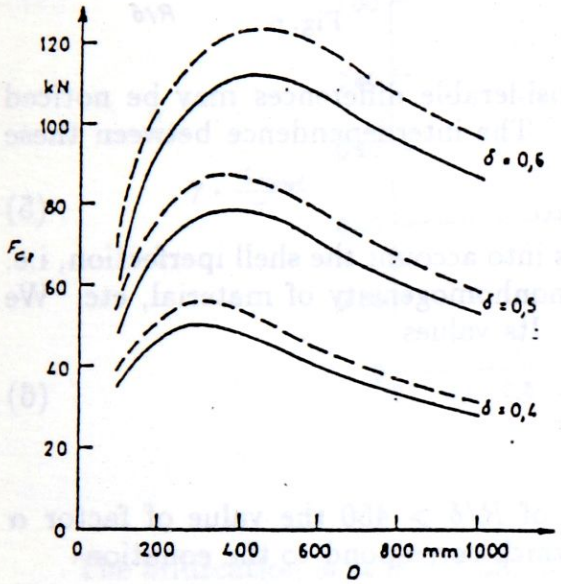


Fig. 3

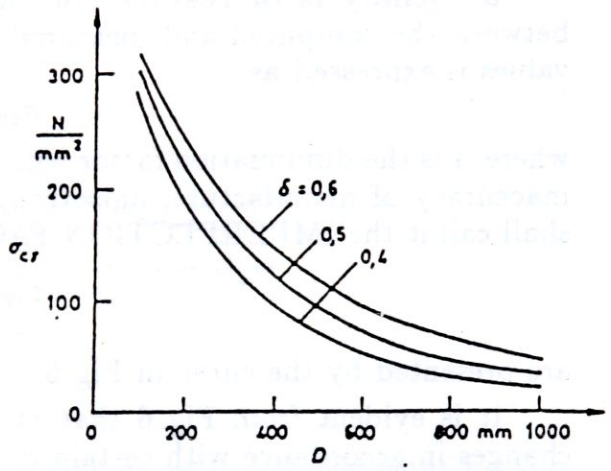


Fig. 4

Although the shells have been carefully manufactured with only minimum deviations from geometrical shape, there are differences between the measured critical forces with shells of the same dimensions. The differences are even up to 10%. In Fig. 3 the full curve presents the lowest measured values and dotted curve the highest values. In the area between these two curves are other measured values. In continuation we shall use the lower curves.

Fig. 4 illustrates the corresponding critical stresses:

$$\sigma_{cr} = \frac{F_{cr}}{D\pi\delta}, \tag{3}$$

where $F_{cr}$ is the lowest value of critical force among five different measured values on shells having the same diameter and wall thickness.

Fig. 5 presents the critical stress curve $\sigma_{cr}$ in relation with the dimensionless factor $R/\delta$. Given is also the ideal critical stress curve obtained through computation upon the classical theory [2]

$$\sigma_{ccr} = 0.605\delta/R. \tag{4}$$

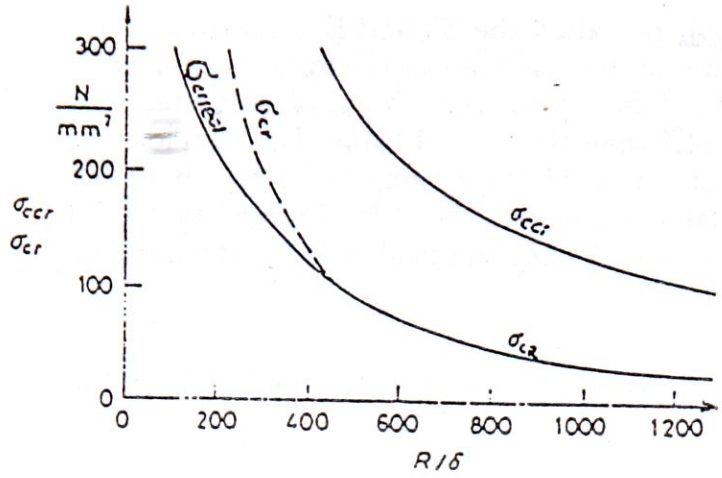


Fig. 5

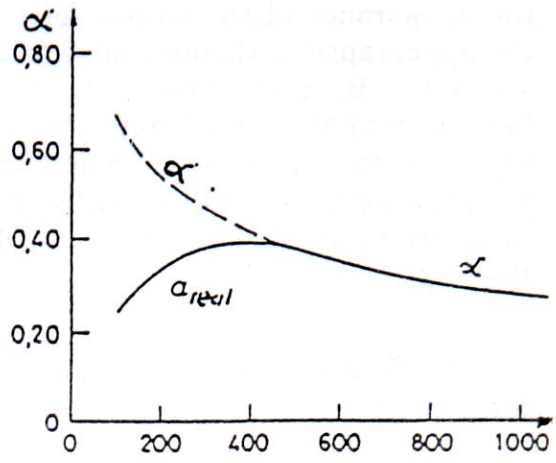


Fig. 6

**5. Analysis of results.** In Fig. 5 considerable differences may be noticed between the computed and measured values. The interdependence between these values is expressed as

$$\sigma_{cr} = \alpha \sigma_{ccr} \tag{5}$$

where $\alpha$ is the diminuation factor which takes into account the shell iperfection, i.e. inaccuracy of manufacture, anisotropy and nonhomogeneity of material, etc. We shall call it the IMPERFECTION FACTOR. Its values

$$\alpha = \frac{\sigma_{cr}}{\sigma_{ccr}} \tag{6}$$

are presented by the curve in Fig. 6.

It is evident from Fig. 6 that at values of $R/\delta > 450$ the value of factor $\alpha$ changes in accordance with certain criteria which correspond to the equation

$$\alpha = \left( \frac{86.49}{100 + (R/\delta)} \right)^{0.5} . \tag{7}$$

At the value of $R/\delta < 450$ a bifurcation occurs where dotted curve signifies the value of $\alpha$ factor if further computed upon the above formula (7), and the full curve, on the other hand, the real value of factor $\alpha$ ($\alpha$ real) obtained through measurements. This curve corresponds to the equation

$$\alpha_{\text{real}} = 0.047 \left( \frac{R}{\delta} \right)^{0.362} . \tag{8}$$

The same bifurcation is seen also in Fig. 5 where the dotted curve presents the critical stress $\sigma_{cr}$, computed upon the formula (5), and the full curve, however, the measured and/or real critical stresses $\sigma_{\text{crreal}}$.

The tests have shown that the bifurcation is the limit where at $R/\delta > 450$ critical forces cause elastic deformations and at $R/\delta < 450$, on the other hand, plastic deformations. We can see in Fig. 5 that within plastic range

$$\sigma_{\text{crreal}} < \sigma_{cr} \tag{9}$$

and within elastic range

$$\sigma_{\text{crreal}} = \sigma_{cr}. \tag{10}$$

Test results naturally depend also upon the sort of material or upon the plastic limit of material $\sigma_v$. In our case this value is

$$\sigma_v = 270\,\mathrm{N/mm^2}. \tag{11}$$

Write the relation between

$$\beta = \sqrt{\frac{\sigma_v}{\sigma_{cr}}} \quad \text{and} \quad \gamma = \frac{\sigma_{crreal}}{\sigma_v}. \tag{12}$$

In Fig. 7 we see the curve presenting the dependence between the values $\beta$ and $\gamma$.

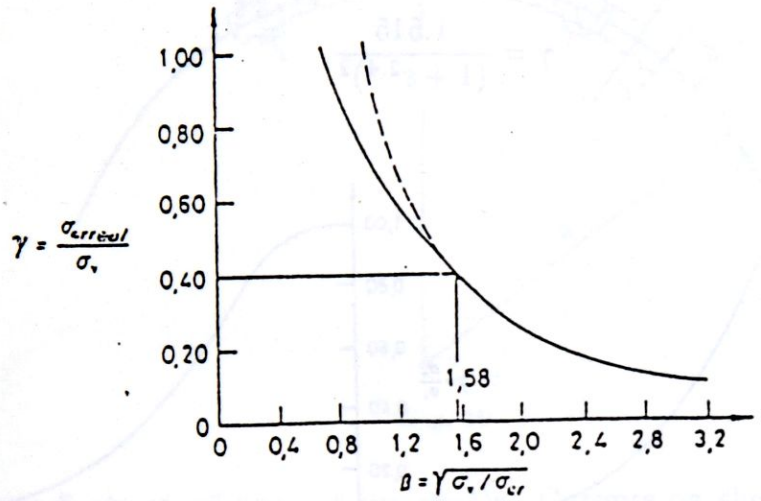


Fig. 7

The bifurcation is at $\beta = 1.58$, i.e. at the point where the critical value reaches

$$\sigma_{cr} = \sigma_{crreal} = 0.4\sigma_v \tag{13}$$

or at $\sigma_{cr} = 108\,\mathrm{N/mm^2}$.

At the value of $\beta > 1.58$ the curve follows the equation

$$\gamma = 1/\beta^2. \tag{14}$$

Within the range of $\beta < 1.58$ there are two stress curves. The dotted curve means the continuation of the expression $\gamma = 1/\beta^2$, whereas the full curve is the one obtained through measurements. The latter corresponds to the equation

$$\gamma = 0.716\beta^{-1.33}. \tag{15}$$

On the basis of the above said we can conclude that without tests it is impossible to make a reliable computation of cylindrical shell critical force. Shells with which critical (buckling) stresses appear within the elastic range have different laws than those shells where such stress appears within the plastic range. This is because the imperfection factor does not equally change within both ranges. We can, therefore, have a uniform criterion for determining the critical stresses of shells of various dimensions through computation only in case when such a criterion does not contain the imperfection factor.

Because of this we shall replace the abscissa $\beta$ in Fig. 7 by a factor called the shell SLENDERNESS

$$\varepsilon = \sqrt{\frac{\sigma_v}{\sigma_{ccr}}}. \tag{16}$$

The experession (16) is a known value since $\sigma_v$ has been determined on the basis of tests carried out in a laboratory and $\sigma_{ccr}$ computed upon a classical method (4). The value of $\sigma_{ccreal}$ in the factor $\gamma$ has been obtained with tests (Fig. 5). In this way the curve in Fig. 8 has been plotted represanting the interdependence of factors $\varepsilon$ and $\gamma$.

This relation may be written in the form of equation

$$\gamma = \frac{1.515}{(1+\varepsilon^{2.4})^2}. \tag{17}$$

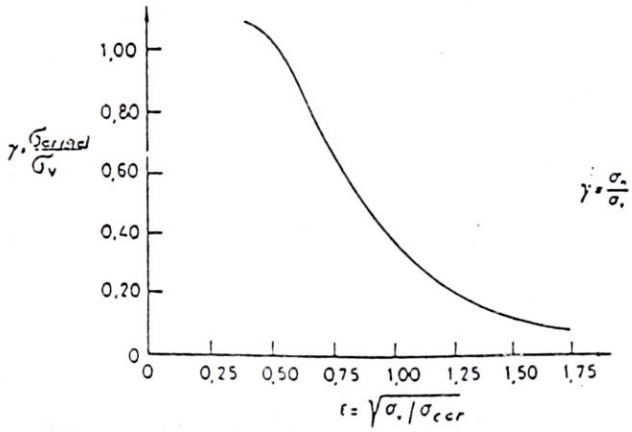


Fig. 8

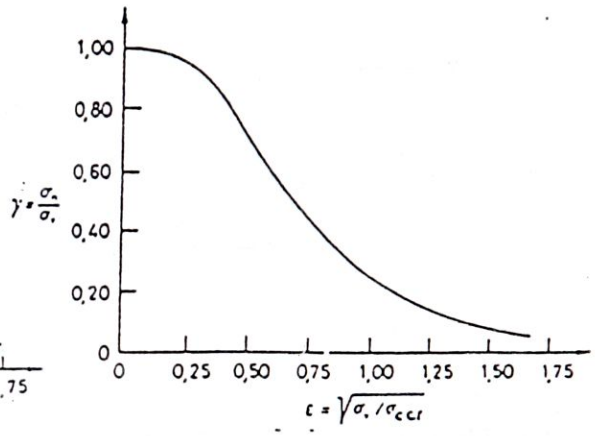


Fig. 9

In practice, however, the shell load $\sigma_n$ must be lower than the critical stress $\sigma_{crreal}$. If we decide that

$$\sigma_n = \frac{\sigma_{crreal}}{1.5} = \frac{\gamma\sigma_v}{1.5} \tag{18}$$

we get a new curve presented in Fig. 9. It can be expressed with the equation

$$\gamma = \frac{1.01}{(1+\varepsilon^{2.4})^2}. \tag{19}$$

The tests have shown that with shells having the slenderness of $\varepsilon > 1$ critical load occurs within the elastic range, with shells of $0.6 < \varepsilon < 1$ within elasto-plastic range and at $\varepsilon < 0.6$ within plastic range.

**6. Effect of unreinforced circular cutouts on circular cylindrical shells buckling under axial compression.** In engineering structures an important role is played by the shells with cutouts.

This paper presents another imperfection — the cutout. A shell with cutout is anisotropic. The cutout causes the displacement of stress trajectories thuscreating

local deviation forces which, even at moderate loads, result in local deformations of shell. It is, therefore, impossible to speak about the stability of shells with cutouts in traditional sense in contrast with shells without cutouts. Exempt are only shells with small cutouts behaving in the same manner as shells without cutouts, under the influence of compression load. The results of experiments made furnish a proof of this phenomenon.

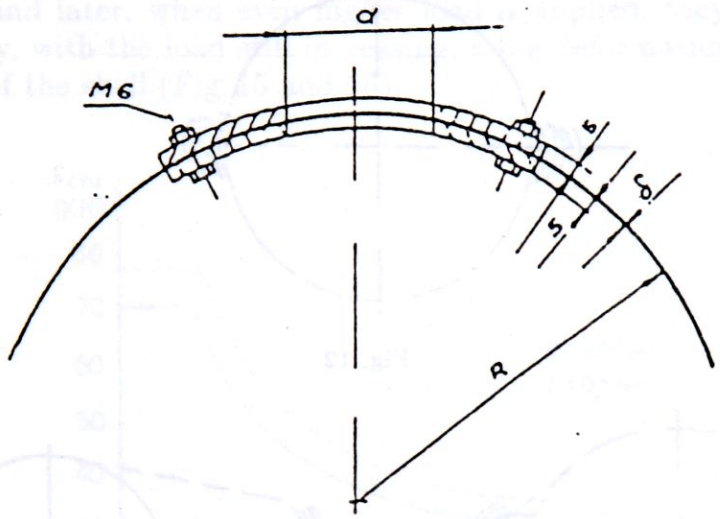


Fig. 10

**7. Manufacture of cutout on shells.** Cutouts on shells were made after annealing in special patterns (Fig. 10)

The pattern consisted of two parts: inner part having the outer radius equal to shell interior radius, and outer part with radius identical to shell outer radius. Both parts had identical cutouts. The shell was fixed between these two parts and the cutout on the shell was cut over the hole on the pattern. After dismantling, the shell with cutout retained the same geometrical shape.

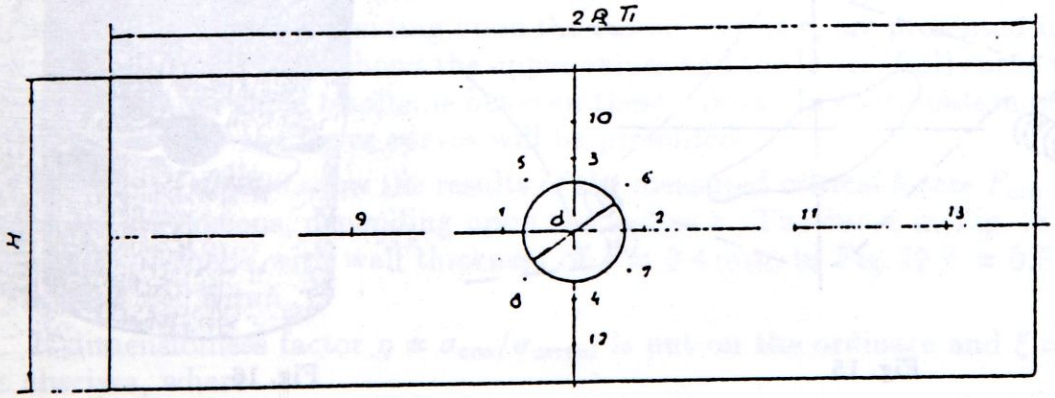


Fig. 11

**8. Test of shell with cutout.** The same testing procedure has been applied as with shells without cutouts. Upon axial compression load the cutout on the shell

acts as a concentrator of stress. The larger the cutout radius the higher the concentration of stress around the cutout and the bigger the deformation. The variations in deformations have been monitored by means of 0.01 precision comparators positioned at several points (Fig. 11). On the basis of the reaction of comparators, the relief of deformations could have been established, especially at the beginning when it was impossible to notice them with the naked eye.

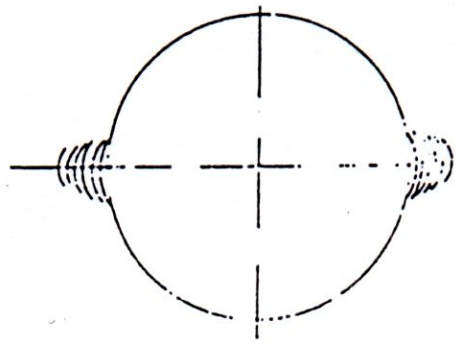

Fig. 12

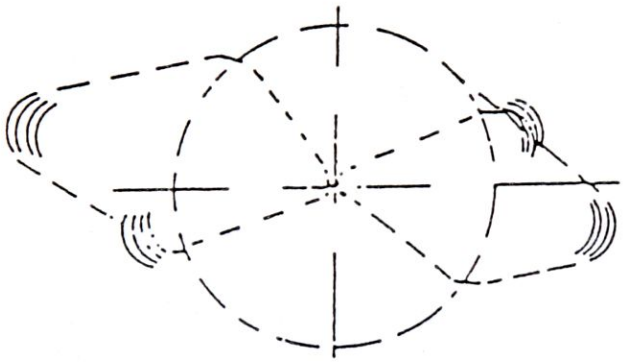

Fig. 13

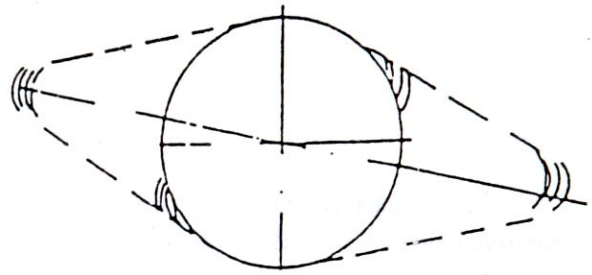

Fig. 14

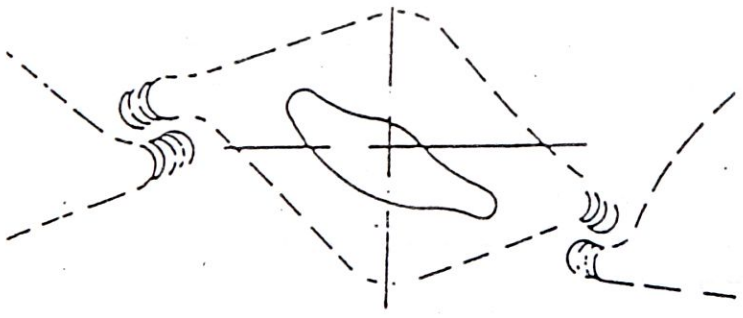

Fig. 15

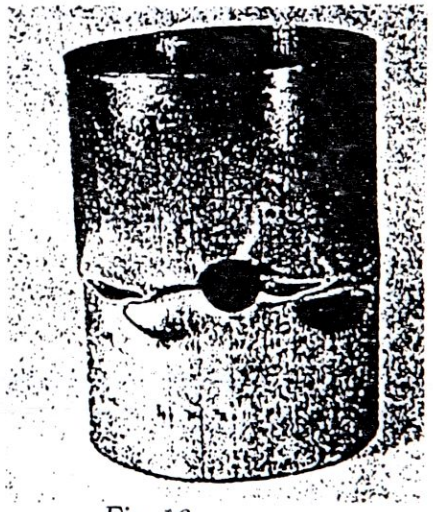

Fig. 16

The tests showed that shells with minor cutouts behaved in the same way as shells without cutouts. At a particular compression force an instantaneous change of the entire plane surface of shell into rhomboidal net was noticed. This compression force shall be called the CRITICAL force.

Shells with larger cutouts behaved differently. The first deformations, appearing as hardly visible bulges, occurred on either side of the cutout (Fig. 12) registered by the comparators 1 and 2. Higher load applied causes an increase in bulges and depressions at points 3 and 4, and later also at 10 and 12. Even the first unsymmetrical deformations result in higher shell imperfection and, as a consequence, in considerable diminishing of shell allowable load.

Through further increase in load the bulges are transformed in two semirhomboids (Fig. 13) and later, when even higher load is applied, they change into one (Fig. 14). Finally, with the load still increasing, a big deformation occurs resulting in the fracture of the shell (Fig. 15 and 16).

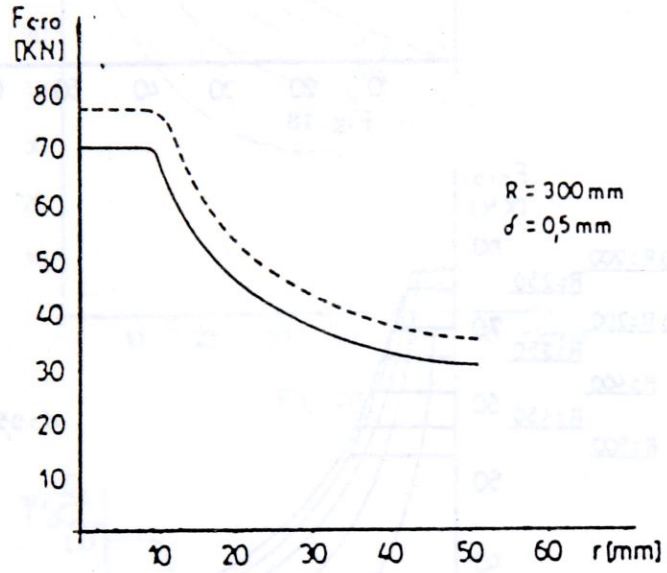


Fig. 17

**9. Test results.** Five samples per each shell of the same dimensions and with identical cutouts were subjected to tests. Despite the fact that the shells were carefully manufactured the values of critical forces differ for up to 10%. As an example, the values of critical forces for the shell with $R = 300\,\text{mm}$ and wall thickness $\delta = 0.5\,\text{mm}$, depending upon the cutout radius $r$, are presented in Fig. 17. The upper (dotted) curve shows the upper values and the lower (full) curve the lower values. The other three results lie between these curves. In continuation of the text in this paper only the lower curves will be presented.

Fig. 18, 19 and 20 show the results of the measured critical forces $F_{cro}$ for shells of various dimensions, depending upon the radius $r$. The curve in Fig. 18 presents the results of shells with wall thickness of $\delta = 0.4\,\text{mm}$, in Fig. 19 $\delta = 0.5\,\text{mm}$ and in Fig. 20 $\delta = 0.6\,\text{mm}$.

If dimensionless factor $\eta = \sigma_{cro}/\sigma_{crreal}$ is put on the ordinate and $\xi = r/R$ on the abscissa, where

$\sigma_{cro} = F_{cro} \cdot A_0$ — critical stress in shell with cutout

$A_0$ — surface of cross-section over cutout

$\sigma_{crreal}$ — real critical stress computed by the formula 12, we get a uniform curve for all shells in Fig. 21.

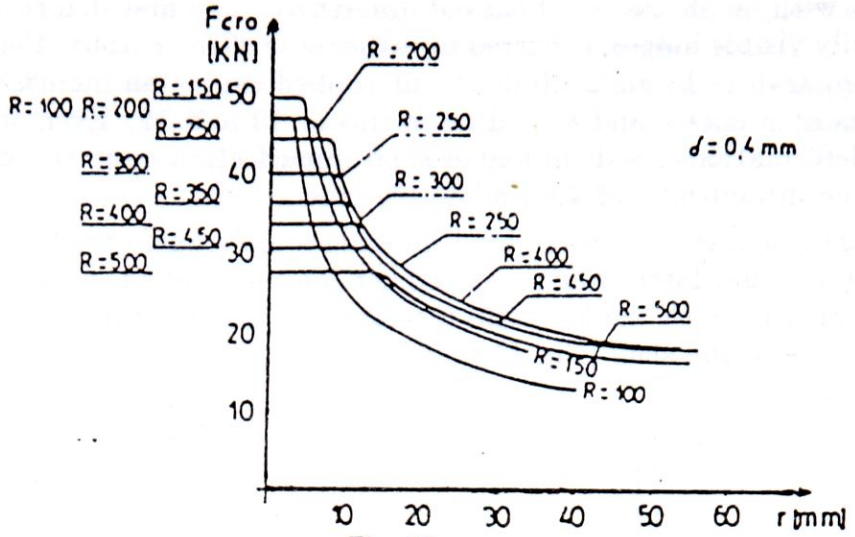


Fig. 18

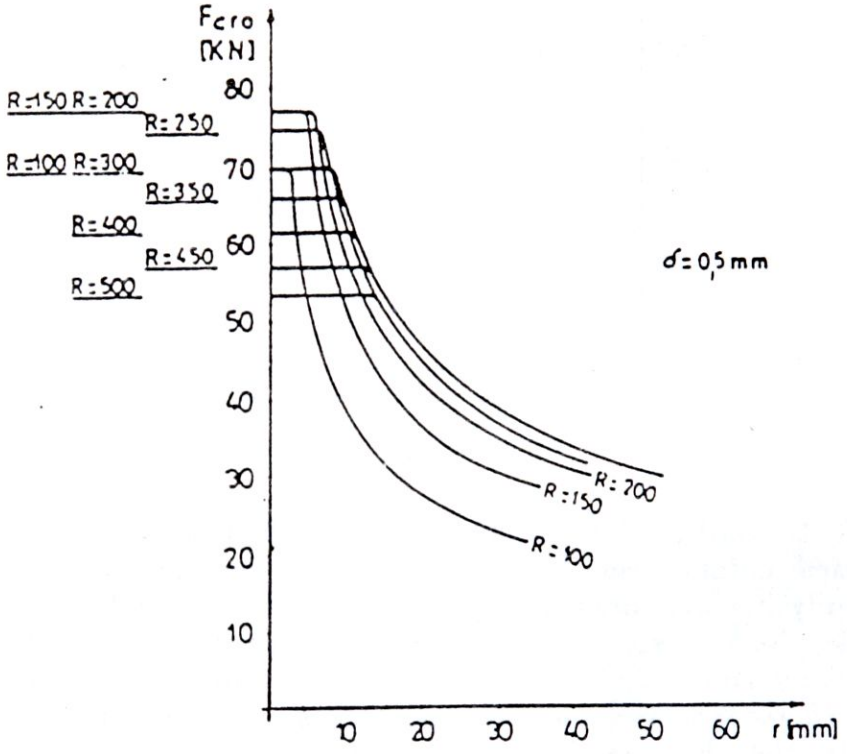


Fig. 19

From the analysis of presented curves a conculusion as follows may be made:

— Shell with a minor cutout behaves as shell without one. Maximum radius of cutout at which the shell behaves as a shell without cutout varies for different shell radii. The larger the shell radii the larger the radius of cutout. Experiments have shown that as a limit value at which the shell with cutout behaves as a shell without it, the relation

$$\frac{r}{R} = 0.028 \tag{20}$$

may be taken. Consequently, with shells of radius $r < 0.028R$ the critical force is the same as with shells without cutout. When the load reaches the value of

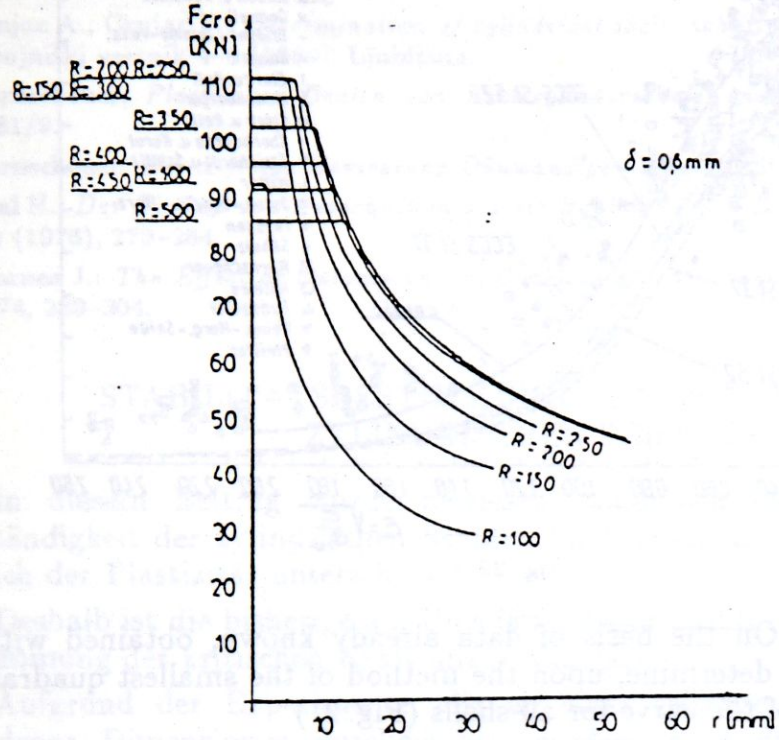


Fig. 20

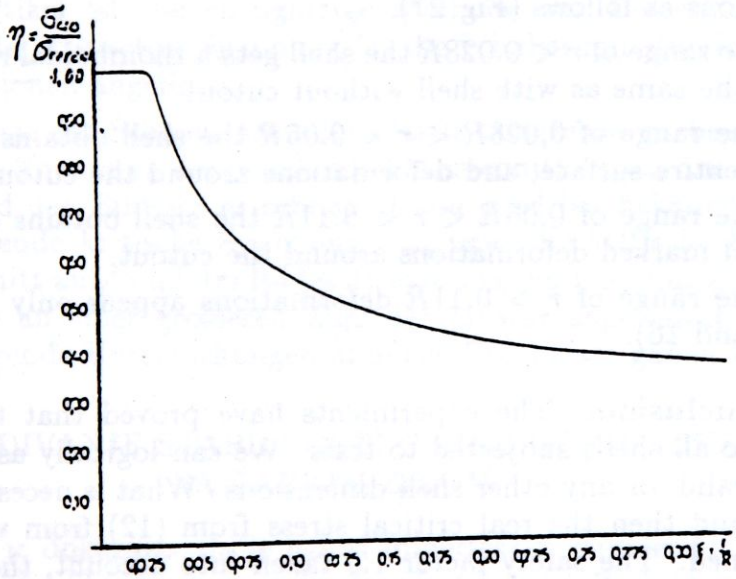


Fig. 21

critical force the same rhomboidal net appears over the entire shell surface as with shells without cutouts. It is to conclude that, the concentration around the cutout is so low that it does not cause the modification of the relief around the cutout.

— With shells having the cutout of $r > 0.028R$, the critical force curve is initially very steep, with an increasing cutout radius, to reach later on a more slightly

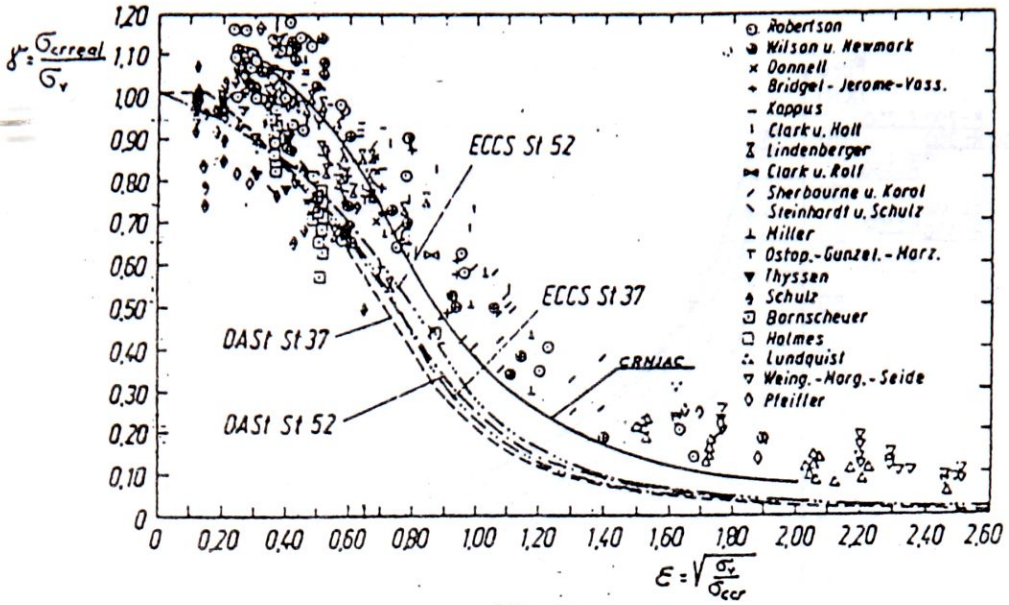


Fig. 22

inclined position. On the basis of data already known, obtained with the tests made, we can determine, upon the method of the smallest quadrants,. a common equation of the curve for all shells (Fig. 21)

$$\eta = 0.197\xi^{-0.456}. \tag{21}$$

The tests have shown that critical force on shells of various dimensions causes the deformations as follows (Fig. 21):

— within the range of $r < 0.028R$ the shell gets a rhomboidal relief ovar the entire surface, the same as with shell without cutout

— within the range of $0.028R < r < 0.05R$ the shell obtains a rhomboidal relif over the entire surface, and deformations around the cutout,

— within the range of $0.05R < r < 0.11R$ the shell obtains a local rhomboidal relief, and marked deformations around the cutout,

— within the range of $r > 0.11R$ deformations appear only around the cutout (Fig. 15 and 16).

**10. Conclusion.** The experiments have proved that the curve in Fig. 8 corresponds to all shells subjected to tests. We can logically assume this curve to be generally valid for any other shell dimensions. What is necessary is to compute $\gamma$ from (17) and then the real critical stress from (12) from which critical force may be obtained. The safety factor 1.5 taken into account, the curve in Fig. 9 is obtained or the expression (19), on the basis of which we can directly compute the allowable load $\sigma_n$ and consequently also the compression force with which the shell may still be loaded.

In this way we would avoid the imperfection factor $\alpha$ and the difficulties related to its determination within both, the elastic and plastic ranges. Subsequent tests should confirm the correcteness of this assumption.

Fig. 22 shows the comparison of the curve CRNJAC (Fig. 8) with the results of the numerouses authors. The curve in Fig. 8 presents the lowest measured values of experiments.

## REFERENCES

[1] Crnjac A., Crnjac P.: *Determination of cylindrical shell stability without imperfection factor*, Strojniški vestnik 4–6 (1989), Ljubljana.

[2] Bornscheuer: *Plastisches Beulen von Kreiszylinderschalen unter Axialbelastung*, Stahlbau 1981/9.

[3] Bornscheuer: *Zur α-freien Bemessung Dünwandiger Schalen*, Stahlbau 85.

[4] Saal H.: *Der Einfluß von Ausschnitten auf die Beullasten von Kreiszylinderschalen*, Stahlbau (9) (1976), 279–284.

[5] Starnes J.: *The Effect of Cutouts on the Buckling of Thin Shells*, In: *Thin Shell Structures*, 1974, 289–304.

## STABILITÄTSBESTIMMUNG VON DÜNNWANDIGEN ZYLINDRISCHEN SCHALEN

In diesem Beitrag wurde bewiesen, dass sich die Einwirkung der Unvollständigkeit der zylindrischen Schalen im Bereich der Elastizität von jener im Bereich der Plastizität unterscheidet.

Deshalb ist die bisherige auf Unvollständigkeitsfaktor $\alpha$ basierende Art für die Bestimmung der kritischen Kraft unzuverlässig.

Aufgrund der Experimente, die an einer grösseren Zahl der Muster verschiedener Dimensionen durchgeführt wurden, wird die einzigartige Methode zur Bestimmung der kritischen Kraft der zylindrischen Schalen, ohne den Unvollständigkeitsfaktor $\alpha$ zu berücksichtigen, angewandt.

In diesem Artikel ist die einzigartige Methode zur Berechnung der kritischen Kraft bzw. der kritischen Spannung für die Schalen mit Rundausschnitt verschiedener Dimensionen angeführt.

Da das Material der Schalen bzw. die Plastizitätsgrenze $\sigma_v$ bekannt ist, wird zuerst die kritische Spannung der Schale ohne Ausschnitt $\sigma_{crreal}$ aus der Gleichung (15) bzw. aufgrund des Bildes 8 errechnet. Dann wird bei bekanntem Verhältnis $r/R$ die entsprechende kritische Spannung $\sigma_{cro}$ bzw. die kritische Kraft $F_{cro}$ der Schale mit Ausschnitt aufgrund des Bildes 21 bzw. aus der Gleichung (21) errechnet. Da diese Methode an einer grösseren Zahl der Muster angewandt wurde, ist zu erwarten, dass folgende Untersuchungen ähnliche Ergebnisse gaben werden.

## ODREĐIVANJE STABILNOSTI CILINDRIČKIH LJUSKI SA TANKIM ZIDOM

U ovom radu je dokazano, da je uticaj imperfekcije cilindričkih ljuski različit u području elastičnosti od onoga u području plastičnosti. Radi toga je nepouzdan dosadašnji način određivanja kritične sile, koji bazira na faktoru imperfekcije $\alpha$.

Na osnovu eksperimenata na velikom broju uzoraka raznih dimenzija, daje se jedinstvena metoda za određivanje kritične sile cilindričkih ljuski, ne uzimajući u obzir faktor imperfekcije $\alpha$.

U ovom članku je prikazana jedinstvena metoda za izračunavanje kritične sile odnosno kritičnog napona, za ljuske sa okruglim otvorom različitih dimenzija.

Pošto je poznat material ljuske odnosno granica plastičnosti $\sigma_v$, najprije izračunamo iz jednadžbe (15), odnosno iz slike 8, kritični napon ljuske bez otvora

$\sigma_{crreal}$. Pri poznatom odnosu $r/R$ zatim izračunamo iz sl. 21, odnosno jednadžbe 21, odgovarajući kritični napon $\sigma_{cro}$ odnosno kritičnu silu $F_{cro}$ ljuske sa otvorom. Pošto ova metoda bazira na većem broju uzoraka, može se očekivati, da će dalja ispitivanja dati slične rezultate.

Ante Crnjac
Peter Crnjac
Technical Faculty,
University of Maribor
62000 Maribor, Yugoslavia